Investigation of LD-slag as oxygen carrier for CLC in a 10 kW unit using high-volatile biomasses

International Journal of Greenhouse Gas Control 127 (2023) 103940

Contents lists available at ScienceDirect

International Journal of Greenhouse Gas Control

journal homepage: www.elsevier.com/locate/ijggc

Investigation of LD-slag as oxygen carrier for CLC in a 10 kW unit using high-volatile biomasses

Daofeng Mei [a,*], Ivan Gogolev [a], Amir H. Soleimanisalim [b], Anders Lyngfelt [a], Tobias Mattisson [a]

[a] Division of Energy Technology, Department of Space, Earth and Environment, Chalmers University of Technology, Gothenburg 41296, Sweden
[b] Biorefinery and Energy Department, RISE Research Institutes of Sweden, Gothenburg 41258, Sweden

ARTICLE INFO

Keywords:
CO_2 capture
Chemical looping combustion
Biomass
Bio-CLC
LD-slag

ABSTRACT

A steel slag from the Linz-Donawitz process, called LD-slag, having significant calcium and iron-fractions, was investigated as an oxygen carrier in a recently developed 10 kW_{th} chemical-looping combustor with three high-volatile biomass fuels. In order to improve operability, the LD-slag was found to require heat-treatment at high temperatures before being used in the unit. In total, operation with the biomasses was conducted for more than 26 h at temperatures of 870–980 °C. The fuel thermal power was in the range of 3.4–10 kW_{th}. The operation involved chemical looping combustion (CLC), chemical looping gasification (CLG) and oxygen carrier aided combustion (OCAC). Around 12 h was in CLC operation, 13.3 h was conducted in CLG-conditions, while the remaining 0.7 h was OCAC. Here, the results obtained during the CLC part of the campaign is reported. Increased temperature in the fuel reactor and higher airflows to the air reactor both lead to better combustion performance. Steam concentration in the fuel reactor has little effect on the performance. The LD-slag showed higher oxygen demand (31.0%) than that with ilmenite (21.5%) and a manganese ore (19.5%) with the same fuel and normal solids circulation. However, with the LD-slag, there is possibility to achieve a lower oxygen demand (15.2%) with high solids circulation.

1. Introduction

Chemical looping combustion (CLC) (Lyngfelt et al., 2001) is a novel combustion technology for thermal and power generation. In CLC, in contrast to conventional combustion, the oxygen for combustion is transferred by oxygen carrier, which is usually composed by oxides of transition metals (Adanez et al., 2012). The oxygen carrier is reduced in a fuel reactor where the fuel is oxidized by the oxygen provided by the oxygen carrier, which is then re-oxidized by oxygen from air in an air reactor. In this way, fuel and air mixing is avoided, thus the fuel reactor gas is not diluted by air N_2, and ideally only H_2O and CO_2 are present in the outlet stream from fuel reactor. The CO_2 can be easily captured after simple steam condensation, which doesn't need intensive energy input, making CLC a promising CO_2 capture technology.

Finding suitable oxygen carrier is crucial for the CLC development, and over 2000 oxygen carriers, either from synthesis, natural ores, or industrial byproducts, have been tested (Abuelgasim et al., 2021). For solid fuels, low-cost materials such as natural ores and industrial by-products are preferred, as the ash from combustion has to be removed from the fuel reactor in large-scale CLC systems. This will inevitably lead to losses of oxygen carrier, and consequently add the operational cost. A number of low-cost naturally occurring materials have been tested for their viability in CLC, which include operations of >1524 h with ilmenite, >1075 h with iron ore, >735 h with manganese ore and >75 h with $CaSO_4$ based oxygen carriers (Mei et al.,). Recently, some industrial byproducts appeared as interesting candidates for CLC, as these materials are normally cheaper than natural ores. Among them, a steel industry byproduct called LD-slag emerges as a promising oxygen carrier (Moldenhauer et al., 2020). The LD-slag is from the Linz-Donawitz process for steel production, and it is available in significant amounts globally and in Sweden at low price. Because of its composition, the LD-slag material has been tested for Chemical Looping Gasification (CLG) process, which converts fuel to syngas (Lin et al., 2020) instead CO_2 in CLC. The LD-slag has presented capability of oxygen transfer to fuel, catalysis of water-gas shift, as well as ability to fix CO_2 through carbonation (Hildor et al., 2020). As compared to ilmenite, the LD-slag showed lower methane conversion and less resistance against attrition. However, the capability of gaseous O_2 release, so-called chemical looping with oxygen uncoupling (CLOU) (Mei et al., 2013; Mattisson et al., 2009), and the low cost as an industrial waste

* Corresponding author.
E-mail address: daofeng.mei@chalmers.se (D. Mei).

https://doi.org/10.1016/j.ijggc.2023.103940
Received 21 February 2023; Accepted 10 July 2023
Available online 20 July 2023

make this material promising for CLC (Hedayati et al., 2022). After operation with fuel, the CLOU property was found to increase and an almost full conversion of CO to CO_2 was achieved (Moldenhauer et al., 2018). In comparison with other Ca- and Mg-rich waste materials (e.g. blast furnace slag and blast furnace dust) and hematite, LD-slag has better reducibility and cyclic stability (Niu and Shen, 2021). LD-slag was used with biomass fuels in a 1.5 kW_{th} unit (Condori et al., 2021), where high-quality syngas and low tar generation were achieved, as well as in a 10 kW_{th} pilot (Moldenhauer et al., 2020). The concept of CLG with LD-slag has been proven with biomasses in a 2–4 MW_{th} gasifer, and the tar yield was found to decrease greatly (Pissot et al., 2018). In addition, LD-slag was reported more magnetic than ilmenite (Karlsson, 2019), and this encourages the use of LD slag in CLC, because the magnetism can facilitate separation of oxygen carrier from ash.

In this work, an LD-slag is studied for its CLC performance with biomass fuels in new, upgraded version of a 10 kW_{th} unit for solid fuels (Gogolev et al., 2022). The experiments were carried out with three high-volatile biomass fuels under various operation conditions. The effect of temperature, solids circulation, steam concentration was evaluated. Composition and microstructure of the LD-slag samples before and after the campaign was analyzed through XRD and SEM-EDX characterizations.

2. Experimental

2.1. Oxygen carrier and fuels

2.1.1. LD-slag oxygen carrier

The as-received LD-slag is in particle form and has a mass-median diameter of d50=160 μm. Ca and Fe are the major components, and Mg, Si and Mn are also present, see Table 1. The presence of Fe and Ca and the LD-slag's low cost make it an interesting oxygen carrier for chemical looping process, because Fe can transfer oxygen and Ca can absorb CO_2 from combustion (Blamey et al., 2010). The as-received LD-slag and the calcined particles after 2 h under 500 °C and 8 h under 950 °C were tested in the 10 kW_{th} unit. A preliminary test showed that uncalcined material can easily cause operational issues, such as severe clogging in chimney, blocking in gas distributor and bed agglomeration. On the contrary, the calcined LD-slag has less problems and has been successfully used in the campaign in the 10 kW_{th} unit, see the comparison in Section 4.1. The calcined LD-slag, which has $Ca_2Fe_2O_5$, Fe_3O_4 and CaO as the main phases (Section 4.5), was sieved to 125–400 μm before use in the 10 kW_{th}. The volumetric magnetic susceptibility of the calcined particles is $9{\cdot}10^{-5}$ m^3/kg, which is higher than that of ilmenite ($3.4{\cdot}10^{-6}$ m^3/kg), and this means the LD-slag could be more easily separated from ash with magnetic separation method (Lamarca, 2021).

2.1.2. Biomass fuels

High-volatile biomass fuels were used in this work, with the proximate and ultimate analyses shown in Table 2. Black Pellets, or BP, are steam exposed wood pellets and supplied by Arbaflame company in Norway. Pine Forest Residue, or PFR, is pellets of pine wood chips supplied by National Renewable Energy centre (CENER) in Spain. Straw Pellets, or SP, are wheat straw and supplied by Stohfelder in Austria. Before use in the unit, these fuels were crushed and sieved to 0.7–2.8, 0.7–3.0 and 0.7–3.5 mm for BP, PFR and SP, respectively. The main property of these biomasses is their high volatiles content ranging from 69.3 to 80%, while the carbon concentration is in the range of 43.2–49.8%. The lower heating value (LHV) of the fuels is 15.8–18.6 MJ/kg. A characteristic number of the fuels is the theoretical oxygen ratio Φ_0 which is defined as the stoichiometric moles of O_2 needed per mole of carbon in the fuel for full combustion (Mei et al., 2021). The PFR needs slightly more O_2 per carbon (Φ_0=1.08), but the fuels have quite similar Φ_0 values, as shown in Table 2.

Table 1
Main elements in the LD-slag (weight percentage,%).

Ca	Fe	Mg	Si	Mn
32	17	5.9	5.6	2.6

2.2. The 10 kW_{th} pilot and operation conditions

The pilot unit has a nominal fuel throughput of 10 kW_{th} for CLC and was recently modified (4) to provide better contact between volatiles and oxygen carrier. Thus, the unit is believed to provide better and more relevant data for operation with high-volatile fuels. As seen in Fig. 1, the unit is mainly composed by fuel feeding system, fuel reactor, air reactor, two loop seals (LS1 and LS2) and two filters (Filter 1&2). Inside the fuel reactor is a volatiles distributor which was added to the new version of the 10 kW_{th} pilot, to improve the contact between bed material and volatiles (Gogolev et al., 2022; Li et al., 2021; Li et al., 2022). The water seal downstream the FR chimney is used to balance the pressure of the system. Pressure transducers are placed along the reactor to monitor the fluidization state and to detect clogging in the reactors. More details of the 10 kW_{th} unit can be found elsewhere (4). In total, 23 kg LD-slag was filled into the system before the campaign and several kilos were added during the operation to compensate the loss due to attrition and elutriation. The main part of the LD-slag bed was in the fuel reactor while the rest was moving among the air reactor, loop seals and riser to maintain circulation state (Linderholm et al., 2012). In the operations, the fuel reactor is fluidized with steam and the air reactor uses air as the fluidization/oxidizing gas. The fuel enters the fuel reactor through a fuel chute with the help of a screw feeder and a flow of sweep N_2 gas. After reactions in the fuel reactor, the gas leaves the fuel reactor via the FR chimney and a part of the gas is pumped to a gas analyzer (NGA 2000, Rosemount ™) to measure the concentration of CH_4, CO, H_2, CO_2 and O_2. The reduced oxygen carrier is circulated, via the LS1 and LS2, between the fuel and air reactors. Exhaust gas from the air reactor is led to the filters to remove elutriated particles before being sent to the stack. The air reactor gas is analyzed by an online analyzer (SIDOR, SICK Sensor Intelligence) to determine the concentration of CO, CO_2 and O_2. All the data are registered in a computer connected to data logger.

In total, around 26 h of operation was conducted under CLC, CLG and OCAC conditions. This paper focuses on 12 h of CLC operation. Operation conditions are compiled in Table 3. The CLC experiments (CLC1–4) were carried out to study the performance of LD-slag with different biomasses at various temperatures (870, 920, 970, 980 and 984 °C), various air flows to the air reactor and also to study the effect of fluidization with H_2O or a mixture H_2O and N_2.

2.3. Characterization techniques

The crystal phase of LD-slag samples was analyzed with the X-ray diffraction (XRD) technique (Bruker D8 Advance). The scanning was performed in the range of 2θ=10–90° with a step size of 0.05°. Proximate and ultimate analyses of the biomasses were analyzed following ISO standard methods [(International Organization for Standardization (ISO) 2017; International Organization for Standardization (ISO) 2015; International Organization for Standardization (ISO) 2015; International Organization for Standardization (ISO) 2016; International Organization for Standardization (ISO) 2015; International Organization for Standardization (ISO) 2017)]. Elements in the LD-slag were determined with the ICP-OES technique (PerkinElmer® Optima 8300) following a modified ASTM D3682 method (ASTM International 2013). To study the morphology inside the particles, the fresh and used samples were dispersed in epoxy resin, modulated, cut, and polished to expose the cross-sectional part and used in the SEM-EDX (Phenom-World) characterization. Magnetic susceptibility of the oxygen carrier samples was determined with a magnetometer (Bartington® MS2B sensor).

Table 2
Analysis of the three biomass fuels.

	Proximate (wt.%, ar)				Ultimate (wt.%, ar)				LHV (MJ/kg)	Φ_0
	FC	V	M	A	C	H	S	N		
BP	18.7	74.2	6.9	0.3	49.8	5.6	0	0.1	18.6	1.06
PFR	9	80	9.2	1.8	46.9	5.7	0.1	0.3	18	1.08
SP	17.1	69.3	8.1	5.5	43.2	5.2	0.1	0.6	15.8	1.04

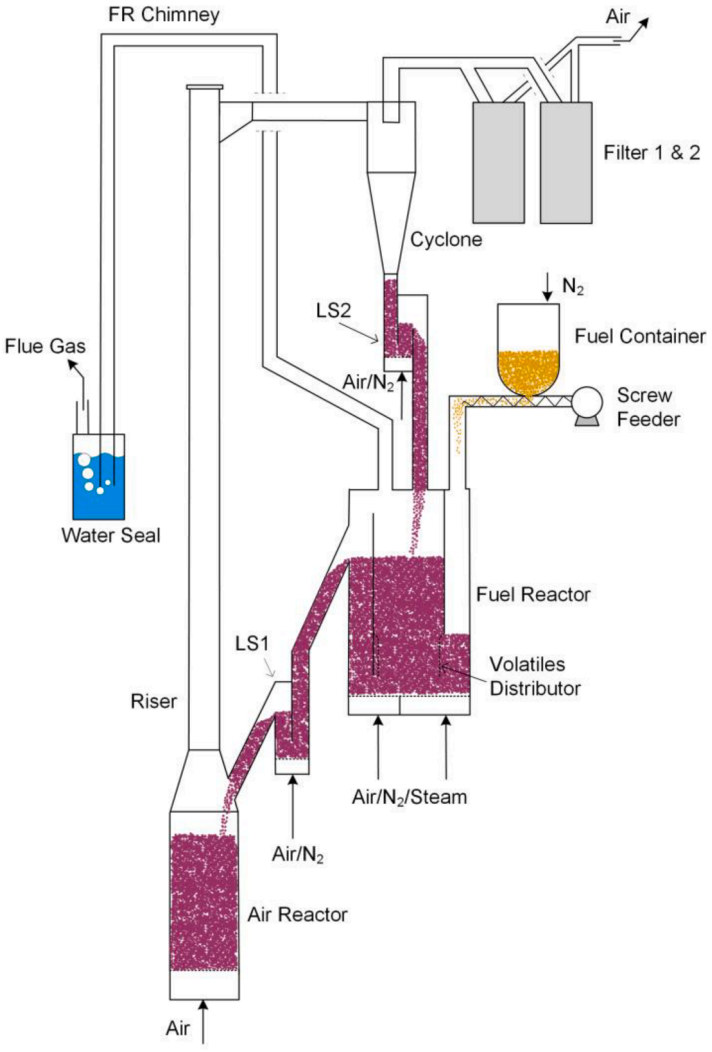

Fig. 1. Schematic description of the 10 kW_{th} CLC pilot.

Table 3
Operation conditions for CLC in this work.

Series	Fuel	T_{FR} (°C)	FR gas	AR flow (L_N/min)	CI (kPa•(L_N•min^{-1}))	Fuel power (kW_{th})	Duration (min)
CLC1	BP	870, 920, 970	H_2O	105–215	264–754	4.6–6.6	322
CLC2	BP	970	H_2O+N_2	215	815–1118	4.6	16
CLC3	PFR	870, 920, 970, 980, 984	H_2O	135–180	387–755	3.8–5.8	141
CLC4	SP	870, 920, 970	H_2O+N_2	105–180	298–426	3.3–5.0	227

3. Data evaluation

Using the fuel-reactor gas concentration $x_{i,FR}$ (i=CO, CH_4, H_2 or CO_2), a dimensionless oxygen demand (Ω_{OD}) can be calculated through Eq. (1) (Berguerand and Lyngfelt, 2009). This parameter represents the theoretical ratio of O_2 required for fully oxidizing the residual gaseous combustibles from the fuel reactor in relation to the oxygen needed for full combustion of the solid fuel.

$$\Omega_{OD} = \frac{0.5x_{CO,FR} + 2x_{CH_4,FR} + 0.5x_{H_2,FR}}{\Phi_0\left(x_{CO,FR} + x_{CH_4,FR} + x_{CO_2,FR}\right)} \quad (1)$$

where Φ_0 is the stoichiometric moles of O_2 needed per mole carbon for

fuel full combustion, cf. Table 2.

The carbon capture (η_{CC}) (Gogolev et al., 2021) is derived from the gas concentrations at the air reactor exit.

$$\eta_{CC} = \frac{x_{O_2,ini} - x_{O_2,AR} - x_{CO_2,AR}}{x_{O_2,ini} - x_{O_2,AR} - 0.21x_{CO_2,AR}} \quad (2)$$

where $x_{O2,ini}$ represents the initial O_2 concentration at the outlet of air reactor before fuel operation, $x_{O2,AR}$ and $x_{CO2,AR}$ are the measured concentrations of O_2 and CO_2 at the outlet of air reactor during fuel operation.

Oxygen carrier circulation rate in the 10 kW_{th} unit cannot easily be measured, but it can be reflected with an index called circulation index (CI). The circulation index CI having a unit of kPa•(L_N•min^{-1}) is calculated through Eq. (3) (Berguerand and Lyngfelt, 2008).

$$CI = \Delta P_{riser} F_{AR,out} \frac{T_{AR} + 273}{273} \quad (3)$$

where the ΔP_{riser} (kPa) is the pressure drop over the riser, $F_{AR,out}$ (L_N•min^{-1}) is the normalized gas flow leaving the air reactor, which is calculated from the inlet air flow and the measured oxygen concentration, T_{AR} (°C) is the air reactor temperature.

4. Results and discussion

4.1. Relevance of LD-slag calcination

The uncalcined LD-slag was first used in the 10 kW_{th} system. However, many issues of clogging and blocking in the reactor chimney and tubes arose during these tests. As an example, Fig. 2a shows the rapid rise in pressure in the fuel reactor chimney as the clogging happened. The elutriated bed material had built up in the horizontal part of the chimney, and this increased the pressure drop over the chimney and blocked the path for gas leaving the reactor, as seen in Fig. 2a. The clogging which happened frequently with the uncalcined LD-slag further led to unstable operation with frequent stops and chimney cleanings. Since the operation with uncalcined LD-slag was not stable, calcined LD-slag was used instead. As seen Fig. 2b, the calcined LD-slag showed much better performance without clogging in the system during a 7 h of continuous operation. The reason for the clogging with uncalcined LD-slag is not fully understood. However, it is clear that the high temperature heat-treatment made stable operation possible. Below, results with the calcined LD-slag are presented.

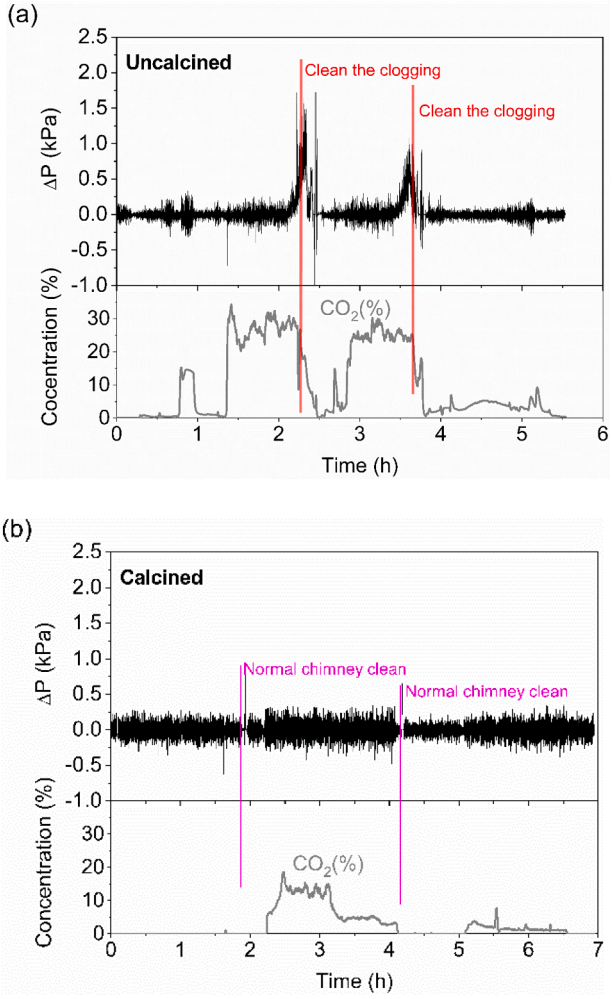

Fig. 2. Comparison of fuel-reactor chimney pressure drop using (a) uncalcined and (b) calcined LD-slag as the bed materials. Red/pink vertical lines show cleaning of chimney. The CO_2 concentration is from fuel reactor and indicates the periods of fuel addition.

4.2. Reaction progress with the calcined LD-slag

Fig. 3 depicts operation in the CLG mode and CLC mode, as well as the transition from CLG to CLC mode. The CLG was shifted to CLC by increasing the air flow to air reactor, which accelerated the oxygen carrier circulation between the two reactors, providing more oxygen for the fuel (Linderholm et al., 2017; Abad et al., 2013). The main gasses leaving the fuel reactor are CO_2, CO, H_2 and CH_4. CLG operation is characterized by CO and H_2 having concentrations above 10%. As the air flow was raised to obtain CLC mode the CO_2 increased, while CO and H_2 decreased and eventually fell below 5%.

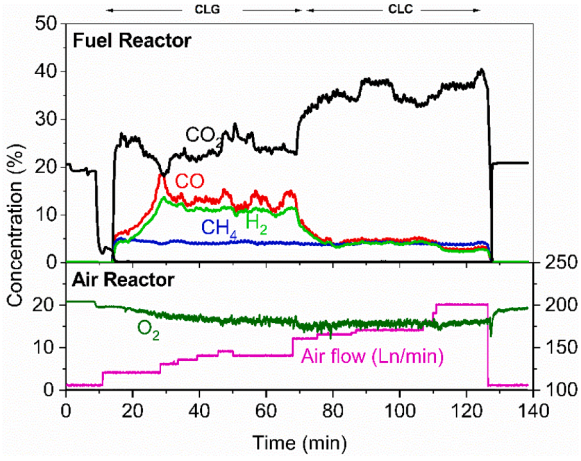

Fig. 3. CLG and CLC operation with BP at 970 °C. Data from series CLC1.

4.3. Effect of operation conditions on CLC

4.3.1. Fuel reactor temperature

As seen in Fig. 4, the increase of fuel reactor temperature improves combustion performance, i.e. the oxygen demand and carbon capture efficiency. For both the BP and PFR fuels, the carbon capture is always higher than 96%, which means less than 4% of the fuel carbon was transported to the air reactor, and this part would not have been captured in the CLC process. When the temperature was increased, the carbon capture efficiency increased to 99% for PFR fuel. At the same time, the oxygen demand was reduced from 52% to 13% at the best. In a real-world application of CLC, oxy-polishing injecting O_2 downstream the fuel reactor to reach full conversion of the fuel would be used (Mei et al., 2021). The very low fuel conversions of around 50% reached was a

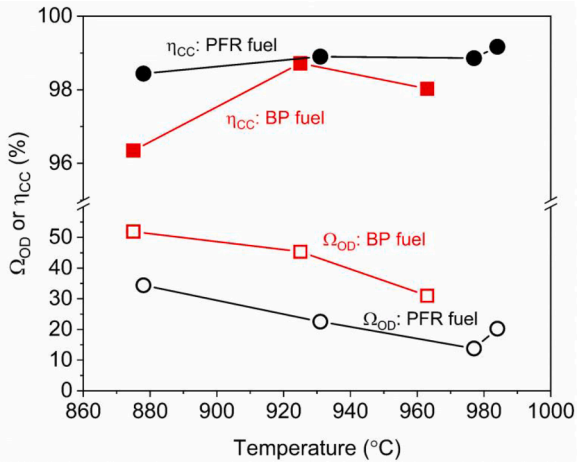

Fig. 4. Effect of fuel reactor temperature on the oxygen demand (Ω_{OD}) and carbon capture efficiency (η_{CC}) with BP and PFR fuels. Data from series CLC1 and CLC3.

result of both low temperature and low oxygen carrier circulation. Furthermore, BP has higher oxygen demands than PFR in the temperature range studied, although the latter has a higher volatiles content. This can be explained by the higher air flow rate used in the PFR case, resulting in higher solids circulation. But the lowest oxygen demand, around 13% obtained with the PFR at around 980 °C is comparable to results in other continuous CLC units burning biomass fuels (Mendiara et al., 2018; Lyngfelt et al., 2019).

4.3.2. *Air flow to the air reactor*

Fig. 5 shows the effect of the air flow, which controls the oxygen carrier circulation rate (4; Linderholm et al., 2017; Linderholm et al., 2016). The faster oxygen carrier circulation means a higher rate of oxygen transfer from the air reactor and a higher average oxidation degree of oxygen carrier in the fuel reactor, thus providing more oxygen for fuel combustion. In general, the oxygen demand was decreased from 31% to 14% depending on the fuel, as the air flow was changed from 135 to 200 L/min. There was no significant effect of air flow on the carbon capture efficiency which was 99%. Among the fuels, the PFR showed the best performance at a flow of 180 L/min, with an oxygen demand of around 10% and a carbon capture of 99%.

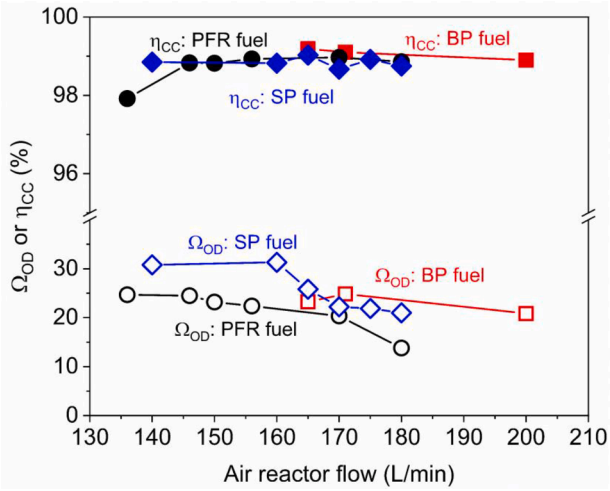

Fig. 5. Effect air reactor flow on the oxygen demand (Ω_{OD}) and carbon capture efficiency (η_{CC}) for BP, PFR and SP fuels. Data from series CLC1, CLC3 and CLC4.

4.3.3. *Steam concentration*

The effect of steam concentration, varying in the range of 20–77% at the fuel reactor inlet, is displayed in Fig. 6 with the BP and SP fuels. The oxygen demand for the BP declined from 17% to 15%, when the steam concentration was increased from 20% to 77%. In the case of the SP fuel, the oxygen demand was decreased from 38% to 31% as the steam was changed from 40% to 77%. A slightly higher carbon capture was also seen at higher steam concentration. A great effect of steam is not expected because of the high volatiles content, which means there is not so much char (around 18%) to be gasified. The much lower oxygen demand, as compared to Figs. 4 and 5, is explained by a very high circulation with a CI of 815–1118 kPa•(L_N•min^{-1}).

4.4. *Comparison with other oxygen carriers*

Data from previous works with ilmenite (Gogolev et al., 2021) and a manganese ore called EB (Elwaleed mine B grade) (4) as oxygen carrier and BP and PFR as fuels are compared with the LD-slag. The carbon capture efficiency for all the three oxygen carriers is the same and as high as 99%, which means very little fuel carbon was transported to the air reactor. On the contrary, the oxygen demand depends on oxygen carriers. Fig. 7 compares the oxygen demand with the three oxygen carriers. With normal CI and the BP fuel, the LD-slag showed a much higher oxygen demand (31%) than ilmenite (21.5%) and EB (19.5%), so the latter two oxygen carriers can convert the fuel better. In the case of PFR, the oxygen demand at normal CI values is similar for the LD-slag and ilmenite, i.e., around 24%. However, with high circulation the oxygen demand for LD-slag is dramatically decreased. Thus, the oxygen demand is 15.2% for a CI of 1118 kPa•(L_N•min^{-1}) with BP and 13.8% for a CI of 896 kPa•(L_N•min^{-1}) with PFR. This large effect of circulation agrees with previous work with LD-slag (Moldenhauer et al., 2020).

4.5. *XRD and SEM-EDX analyses*

As seen in Fig. 8, the phase composition of the fresh calcined LD-slag is very similar to that of the used LD-slag. Thus, both are mainly composed by $Ca_2Fe_2O_5$, some Fe_3O_4 and CaO. This indicates that most of the Ca and Fe are present as $Ca_2Fe_2O_5$, which is also a promising oxygen carrier (Sun et al., 2018). Further, the oxygen carrier composition is stable during the campaign. The magnetic susceptibility of the used LD-slag is $7{\cdot}10^{-5}$ m^3/kg which is similar to the fresh calcined particles and much higher than that of ilmenite, and this indicates that magnetic separation can be used.

SEM-EDX analysis of the fresh calcined and the used LD-slag is shown

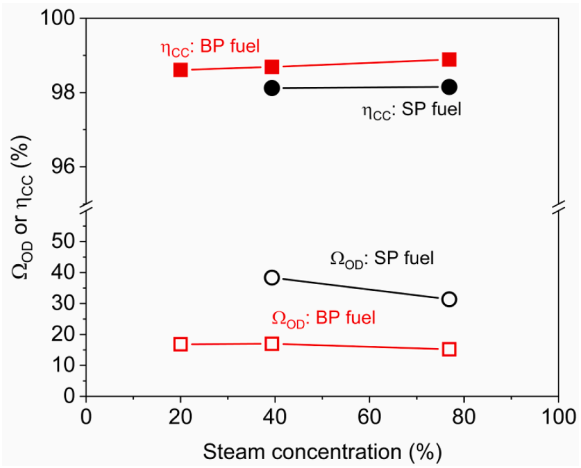

Fig. 6. Effect of steam concentration on the carbon capture (η_{CC}) and oxygen demand (Ω_{OD}) of BP and SP fuels. The steam concentration was varied in the range of 20–77%. Data from series CLC2 and CLC4.

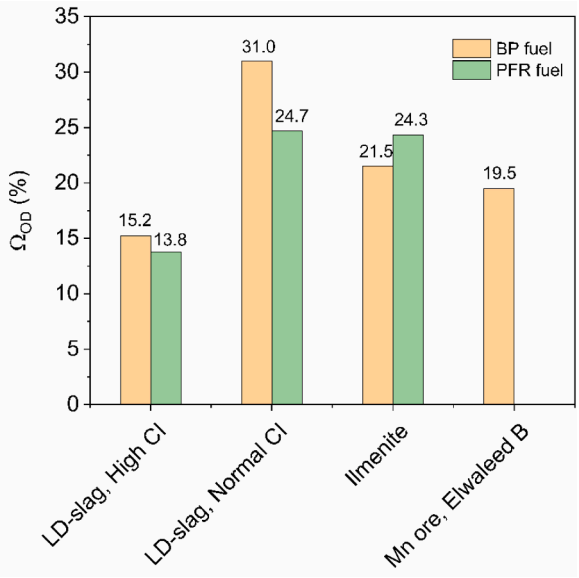

Fig. 7. Oxygen demand in CLC with BP fuel, PFR fuel and LD-slag (both at high CI and normal CI), ilmenite and manganese ore (Elwaleed B) oxygen carriers. The LD-slag's data with PFR is from CLC3, at high CI with BP is from CLC2 and at normal CI with BP is from CLC1, the data for ilmenite is from (Gogolev et al., 2021) and the data for Mn ore is from (4).

in Fig. 9 below. In agreement with the ICP-OES analysis shown in Table 1, the fresh calcined LD-slag has Ca and Fe as the main elements and minor Si, see Fig. 9a-d. After CLC/CLG operations, Fig. 9e-h, there is no agglomeration between particles and an even distribution of Ca, Fe and Si in the cross-section of the particles is also seen, the latter often involved in agglomeration together with alkalis (Mei et al., 2022). No obvious difference is noticed between the fresh calcined and the CLC/CLG used oxygen carrier.

5. Conclusion

For all the three fuels, the carbon capture efficiency is normally higher than 95%, indicating that less than 5% of the fuel carbon was transferred to the air reactor. At higher temperature the fuel conversion was 77–87%, corresponding to oxygen demands of 13–23%. Variations of the steam flow to the fuel reactor slightly influenced CLC performance. The oxygen demand for SP at 970 °C fell from 38 to 33% when steam concentration was increased from 40 to 77%. However, the steam flow had almost no effect when using the BP fuel; the oxygen demand was in a narrow range of 15–17%. The oxygen demand reflects a limited gas-solids contact and an industrial-scale fuel reactor with a high riser similar to circulating fluidized-bed boilers could be expected to have better performance. Under CLC conditions, there was no sign of defluidization or agglomeration, which means that this by-product from the steel industry could be considered for use in CLC with biomass. The fresh and used LD-slag particles kept similar magnetic susceptibility, which indicates good potential of magnetic separation from ash. LD-slag differs from other often examined oxygen carrier materials by being very

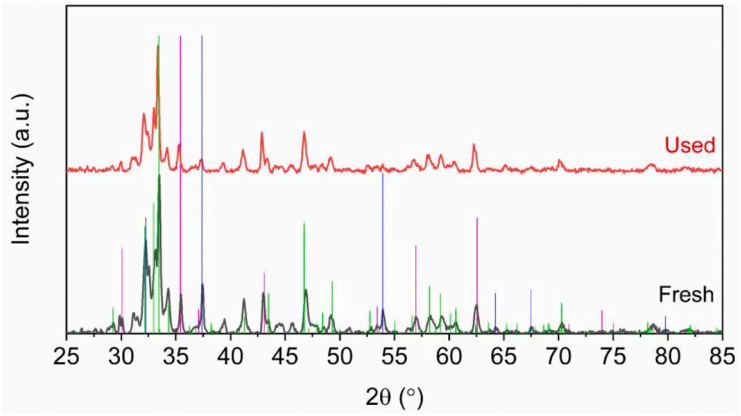

Fig. 8. Identification of XRD compositions for the fresh calcined LD-slag and the used LD-slag samples. The vertical lines represent the standard patterns of $Ca_2Fe_2O_5$ (green), Fe_3O_4 (pink), and CaO (blue).

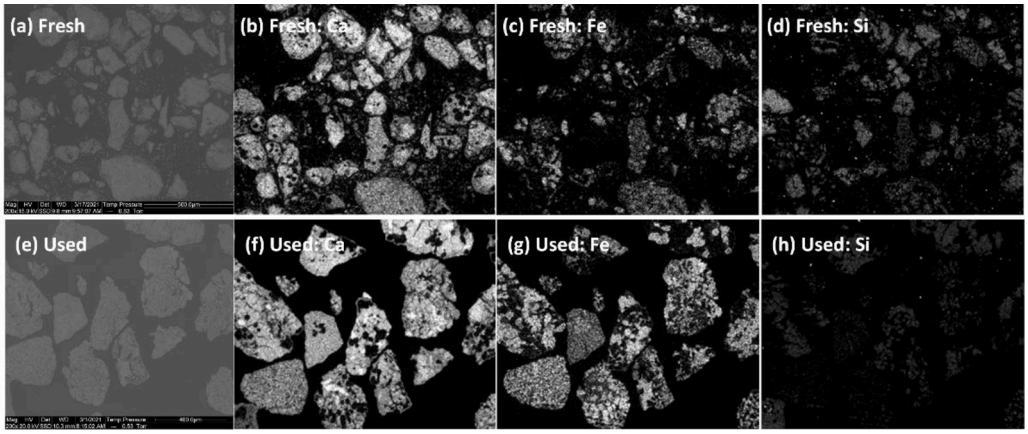

Fig. 9. Morphology and element analyses through the SEM-EDX technique for (a-d) the fresh calcined LD-slag and (e-h) the used LD-slag.

sensitive to circulation. Thus, with moderate circulation performance is poor, but at very high circulation LD-slag is markedly better than comparable materials like ilmenite and a manganese ore.

Declaration of Competing Interest

The authors declare that they have no known competing financial interests or personal relationships that could have appeared to influence the work reported in this paper.

Data availability

Data will be made available on request.

Acknowledgement

This work was carried out with funding from Swedish Research Council, project "Biomass combustion chemistry with oxygen carriers" (contract 2016–06023). The authors are grateful to Carl Linderholm and Fredrik Hildor for their support on the 10 kW_{th} unit operation and material characterizations. This work was presented and benefited from discussions at the "Chemical Looping 2020″ conference (6th International Conference on Chemical Looping in Zaragoza, Spain).

References

Abad, Alberto, Adánez, Juan, de Diego, Luis F., Gayán, Pilar, García-Labiano, Francisco, Lyngfelt, Anders, 2013. Fuel reactor model validation: Assessment of the key parameters affecting the chemical-looping combustion of coal. Int. J. Greenhouse Gas Control 19, 541–551.

Abuelgasim, Siddig, Wang, Wenju, Abdalazeez, Atif, 2021. A brief review for chemical looping combustion as a promising CO_2 capture technology: Fundamentals and progress. Sci. Total Environ. 764, 142892.

Adanez, Juan, Abad, Alberto, Garcia-Labiano, Francisco, Gayan, Pilar, Diego, Luis F.de, 2012. Progress in Chemical-Looping Combustion and Reforming technologies. Progress Energ. Combust. Sci. 38 (2), 215–282.

ASTM International, 2013. ASTM D3682-13-Standard Test Method For Major and Minor Elements in Combustion Residues from Coal Utilization Processes. ASTM International, West Conshohocken, PA.

Berguerand, Nicolas, Lyngfelt, Anders, 2008. Design and operation of a 10 kW_{th} chemical-looping combustor for solid fuels – Testing with South African coal. Fuel 87 (12), 2713–2726.

Berguerand, Nicolas, Lyngfelt, Anders, 2009. Chemical-Looping Combustion of Petroleum Coke Using Ilmenite in a 10 kWth Unit−High-Temperature Operation. Energy & Fuels 23 (10), 5257–5268.

Blamey, J., Anthony, E.J., Wang, J., Fennell, P.S., 2010. The calcium looping cycle for large-scale CO_2 capture. Progress Energ. Combust. Sci. 36 (2), 260–279.

Condori, Oscar, García-Labiano, Francisco, de Diego, Luis F., Izquierdo, María T., Abad, Alberto, Adánez, Juan, 2021. Biomass chemical looping gasification for syngas production using LD Slag as oxygen carrier in a 1.5 kW_{th} unit. Fuel Process. Tech. 222, 106963.

Gogolev, Ivan, Soleimanisalim, Amir H, Mei, Daofeng, Lyngfelt, Anders, 2022. Effects of Temperature, Operation Mode, and Steam Concentration on Alkali Release in Chemical Looping Conversion of Biomass- Experimental Investigation in a 10 kW_{th} Pilot. Energy & Fuels 36 (17), 9551–9570.

Gogolev, Ivan, Soleimanisalim, Amir H., Linderholm, Carl, Lyngfelt, Anders, 2021. Commissioning, performance benchmarking, and investigation of alkali emissions in a 10 kW_{th} solid fuel chemical looping combustion pilot. Fuel 287, 119530.

Hedayati, Ali, Soleimanisalim, Amir H., Mattisson, Tobias, Lyngfelt, Anders, 2022. Thermochemical conversion of biomass volatiles via chemical looping: Comparison of ilmenite and steel converter waste materials as oxygen carriers. Fuel 313, 122638.

Hildor, Fredrik, Leion, Henrik, Linderholm, Carl Johan, Mattisson, Tobias, 2020. Steel converter slag as an oxygen carrier for chemical-looping gasification. Fuel Process. Tech. 210, 106576.

International Organization for Standardization (ISO), 2015. ISO 16948:2015. Solid Biofuels-Determination of Total Content of Carbon, Hydrogen and Nitrogen. ISO, Geneva, Switzerland.

International Organization for Standardization (ISO), 2015. ISO 18123:2015. Solid Biofuels-Determination of the Content of Volatile Matter. ISO, Geneva, Switzerland.

International Organization for Standardization (ISO), 2015. ISO 18122:2015. Solid Biofuels-Determination of Ash Content. ISO, Geneva, Switzerland.

International Organization for Standardization (ISO), 2016. ISO 16994:2016. Solid Biofuels-Determination of Total Content of Sulfur and Chlorine. ISO, Geneva, Switzerland.

International Organization for Standardization (ISO), 2017. ISO 18125:2017. Solid Biofuels-Determination of Calorific Value. ISO, Geneva, Switzerland.

International Organization for Standardization (ISO), 2017. ISO 18134-2:2017. Solid Biofuels-Determination of Moisture Content-Oven Dry Method-Part 2: Total Moisture-Simplified Method. ISO, Geneva, Switzerland.

Karlsson, Frida, 2019. Master's Thesis. Chalmers University of Technology.

Lamarca, Ignacio, 2021. Magnetic Separation of Ilmenite Used As an Oxygen Carrier in Fluidized Bed Combustion. Chalmers University of Technology.

Li, Xiaoyun, Lyngfelt, Anders, Linderholm, Carl, Leckner, Bo, Mattisson, Tobias, 2022. Performance of a volatiles distributor equipped with internal baffles under different fluidization regimes. Powd. Tech. 409, 117807.

Li, Xiaoyun, Lyngfelt, Anders, Mattisson, Tobias, 2021. An experimental study of a volatiles distributor for solid fuels chemical-looping combustion process. Fuel Process. Tech. 220, 106898.

Lin, Yan, Wang, Haitao, Wang, Yonghao, Huo, Ruiqiang, Huang, Zhen, Liu, Ming, Wei, Guoqiang, Zhao, Zengli, Li, Haibin, Fang, Yitian, 2020. Review of Biomass Chemical Looping Gasification in China. Energy & Fuels 34 (7), 7847–7862.

Linderholm, Carl, Lyngfelt, Anders, Cuadrat, Ana, Jerndal, Erik, 2012. Chemical-looping combustion of solid fuels – Operation in a 10 kW unit with two fuels, above-bed and in-bed fuel feed and two oxygen carriers, manganese ore and ilmenite. Fuel 102, 808–822.

Linderholm, Carl, Schmitz, Matthias, Knutsson, Pavleta, Lyngfelt, Anders, 2016. Chemical-looping combustion in a 100-kW unit using a mixture of ilmenite and manganese ore as oxygen carrier. Fuel 166, 533–542.

Linderholm, Carl, Schmitz, Matthias, Lyngfelt, Anders, 2017. Estimating the solids circulation rate in a 100-kW chemical looping combustor. Chem. Eng. Sci. 171, 351–359.

Lyngfelt, Anders, Brink, Anders, Langørgen, Øyvind, Mattisson, Tobias, 2019. Magnus Rydén, Carl Linderholm. 11,000 h of chemical-looping combustion operation—Where are we and where do we want to go? Int. J. Greenhouse Gas Control 88, 38–56.

Lyngfelt, Anders, Leckner, Bo, Mattisson, Tobias, 2001. A fluidized-bed combustion process with inherent CO_2 separation; application of chemical-looping combustion. Chem. Eng. Sci. 56 (10), 3101–3113.

Mattisson, Tobias, Lyngfelt, Anders, Leion, Henrik, 2009. Chemical-looping with oxygen uncoupling for combustion of solid fuels. Int. J. Greenhouse Gas Control 3 (1), 11–19.

Mei, Daofeng, Linderholm, Carl, Lyngfelt, Anders, 2021. Performance of an oxy-polishing step in the 100 kW_{th} chemical looping combustion prototype. Chem. Eng. J. 409, 128202.

Mei, Daofeng, Lyngfelt, Anders, Leion, Henrik, Linderholm, Carl, Mattisson, Tobias, 2022. Oxygen Carrier and Alkali Interaction in Chemical Looping Combustion: Case Study Using a Braunite Mn Ore and Charcoal Impregnated with K_2CO_3 or Na_2CO_3. Energy & Fuels 36 (17), 9470–9484.

Mei, Daofeng, Amir H. Soleimanisalim, Carl Linderholm, Anders Lyngfelt, Tobias Mattisson. Reactivity and lifetime assessment of an oxygen releasable manganese ore with biomass fuels in a 10 kWth pilot rig for chemical looping combustion, Fuel Process. Tech. 215, 106743.

Mei, Daofeng, Zhao, Haibo, Ma, Zhaojun, Zheng, Chuguang, 2013. Using the Sol–Gel-Derived CuO/CuAl2O4 Oxygen Carrier in Chemical Looping with Oxygen Uncoupling for Three Typical Coals. Energy & Fuels 27 (5), 2723–2731.

Mendiara, Teresa, García-Labiano, Francisco, Abad, Alberto, Gayán, Pilar, de Diego, Luis F., Izquierdo, Maria Teresa, Adánez, Juan, 2018. Negative CO_2 emissions through the use of biofuels in chemical looping technology: A review. Applied Energy 232, 657–684.

Moldenhauer, Patrick, Linderholm, Carl, Rydén, Magnus, Lyngfelt, Anders, 2018. Experimental investigation of chemical-looping combustion and chemical-looping gasification of biomass-based fuels using steel converter slag as oxygen carrier. In: International Conference on Negative CO_2 Emissions. Gothenburg, Sweden. May 22-24.

Moldenhauer, Patrick, Linderholm, Carl, Rydén, Magnus, Lyngfelt, Anders, 2020. Avoiding CO_2 capture effort and cost for negative CO_2 emissions using industrial waste in chemical-looping combustion/gasification of biomass. Mitigation and Adaptation Strategies for Global Change 25, 1–24.

Niu, Xin, Shen, Laihong, 2021. Ca- and Mg-rich waste as high active carrier for chemical looping gasification of biomass. Chin. J. Chem. Eng. 38, 145–154.

Pissot, Sébastien, Vilches, Teresa Berdugo, Maric, Jelena, Seemann, Martin, 2018. Chemical looping gasification in a 2-4 MW_{th} dual fluidized bed gasifier. In: Proceedings of the 23rd International Conference on Fluidized Bed Conversion. Seoul, Korea, 13–17 May.

Sun, Zhao, Chen, Shiyi, Hu, Jun, Chen, Aimin, Rony, Asif Hasan, Russell, Christopher K., Xiang, Wenguo, Fan, Maohong, Dyar, M.Darby, Dklute, Elizabeth C., 2018. $Ca_2Fe_2O_5$: A promising oxygen carrier for CO/CH_4 conversion and almost-pure H_2 production with inherent CO_2 capture over a two-step chemical looping hydrogen generation process. Applied Energy 211, 431–442.